DEUTSCHES ELEKTRONEN-SYNCHROTRON **DESY**

DESY 89-047
April 1989

Probing New Contact Interactions at Future pp, ep and e^+e^- Colliders

F. Schrempp

Deutsches Elektronen-Synchrotron DESY

ISSN 0418-9833

NOTKESTRASSE 85 · 2 HAMBURG 52

To be sure that your preprints are promptly included in the
HIGH ENERGY PHYSICS INDEX ,
send them to the following address (if possible by air mail) :

DESY
Bibliothek
Notkestrasse 85
2 Hamburg 52
Germany

DESY 89-047
April 1989

ISSN 0418-9833

Probing New Contact Interactions at Future *pp*, *ep* and e^+e^- Colliders *

Fridger Schrempp

Deutsches Elektronen Synchrotron DESY, D-2000 Hamburg

April 25, 1989

Abstract

A comparative discussion of the 'reach' Λ^* for possible new contact interactions at future *pp*, $e^{\pm}p$ and e^+e^- colliders is presented. First of all, some introductory background is provided concerning the generality of the concept of contact interactions and the interpretation of the associated scale Λ^* . Useful analytical insight comes, moreover, from a simple scaling law and a more specialized approximate formula for the energy and luminosity dependence of Λ^* . In a second part, 'state of the art' numerical simulations for extracting Λ^* are discussed. For e^+e^- collisions, an analysis is reviewed which extends from PETRA/ PEP energies, via the Z^0 peak, up to the TeV regime of a possible linear collider (CLIC). For *pp* and $\bar{p}p$ collisions, a new detailed analysis was performed, extending from $S\bar{p}pS$ energies, via the LHC and SSC regime, up to a possible 200 TeV pp collider (ELOISATRON). The importance of longitudinal beam polarization for filtering out contact interactions is illustrated for the case of HERA and LEP.

1 Introduction

A major objective of experiments at future high energy accelerators will be to search for new particles and interactions announcing the onset of physics beyond the Standard Model.

Although the Standard Model so far perfectly manages to accomodate all existing experimental data, there are a number of well known theoretical arguments, calling for some sort of modification of the present theory, not far above the Fermi scale of weak interactions, $\Lambda_F \simeq 250$ GeV. While in the light of such arguments the appearance of new particles and interactions seems unavoidable, their specific properties entirely depend on the preferred scheme, such as the supersymmetry-superstring pathway[1] or, perhaps, a world with composite quarks and leptons and/or Higgs bosons [2].

*Invited talk delivered at the 7*th* ELOISATRON Workshop, Centro di Cultura Scientifica "Ettore Majorana", Erice-Trapani, Sicily, Italy, June 10-27, 1988

The discovery of dramatic formation peaks or the crossing of new open production thresholds at one of the forthcoming high energy colliders would certainly provide the most unambigous signals of new particles. Yet, the mass range accessible in this case is strictly limited by the available beam energy.

A considerably larger mass range may be explored, however, through the study of effects from *virtual* new particle exchanges. For masses much larger than the beam energy such indirect signatures may be conveniently and model independently investigated by adding general contact interaction terms to the Standard Model lagrangian, quite analogously to Fermi's early description of the weak interactions. The potential of such a strategy was particularly emphasized by Eichten et. al. [3,4,5] and Ref. [6] in the context of quark and lepton substructure. It is important to note, however, that (experimental) limits on the strength of contact interactions provide information on possible new physics in a far more general sense (c.f. Sect. 2.1).

The purpose of this report is to present a comparative discussion of the 'reach' for new contact interactions at the various forthcoming *pp*, *ep* and e^+e^- colliders.

In Sect. 2.1 I shall provide some introductory background concerning the generality of the concept of contact interactions and the interpretation of the associated scale Λ^* . The four-fermion contact interaction terms as relevant for the various types of colliders are then introduced in Sect. 2.2. Useful analytical insight comes from a simple scaling law and a more specialized approximate formula for the energy and luminosity dependence of the 'reach' Λ^* (Sect. 2.3). In Sects. 3 I proceed to discuss selected results from 'state of the art' simulations for the various colliders. I start in Sect. 3.1 with reviewing an analysis of contact interactions at future e^+e^- colliders, which covers the entire energy range from PETRA/PEP up to a possible 2 TeV linear collider (CLIC) under realistic assumptions about expected detector performances and machine luminosities. An important issue in the discussion about future machines concerns the question of beam polarization. In Sect. 3.2 I shall illustrate the impact of longitudinal polarization on contact interactions for the case of HERA and LEP. Finally, Sect. 3.3 deals with a new detailed study of general contact terms for *pp* and $\bar{p}p$ colliders. It covers the entire energy range from the $S\bar{p}pS$ up to a possible 200 TeV pp collider (ELOISATRON). The bounds on Λ^* are extracted from the two-jet angular distribution $\frac{1}{\sigma_{2j}} d\sigma_{2j}/d\chi$ at large two-jet masses which enjoys a number of advantages over previous methods and has been proven at the $S\bar{p}pS$ to be relatively free of systematic errors.

Finally, the results for Λ^* to be expected at the various future colliders are compared to each other in the Conclusions.

2 Reach for Contact Interactions

2.1 Setting the Stage

Including contact interactions both in real experiments and in simulations for future colliders has by now become a standard matter. Yet, since in the literature such a procedure is often *identified* with ideas of quark and lepton substructure, it may be worth spending a few words to point out the actual generality of this (effective lagrangian) method.

The basic assumption is that the Standard Model is, in fact, part of a larger theory,

involving more (heavier) fields besides the ones we know already[1]. At this point it is irrelevant whether the full theory e.g. involves a grand unification of gauge forces, supersymmetry or describes the interactions of quark and lepton constituents. What matters is that at energies small as compared to some characteristic scale $\Lambda > m_W$ the $SU(3)_c \times SU(2)_L \times U(1)_Y$ symmetric Standard Model results to good approximation, after the unobservable fields (particles) have been integrated out. In this case, the total lagrangian, valid up to energies $\sqrt{s} < (<)\Lambda$, may be written in terms of presently *relevant* fields only (quarks, leptons, gluons, W's, γ, Higgs), in form of an expansion in powers of $1/\Lambda$

$$\mathcal{L}_{eff} = \mathcal{L}_{SM} + \frac{1}{\Lambda}\mathcal{L}_5 + \frac{1}{\Lambda^2}\mathcal{L}_6 + \ldots \tag{1}$$

Here, the leading term of mass dimension 4, $\mathcal{L}_{SM}$, is to be identified with the (renormalizable) Standard Model lagrangian. The additional terms $\mathcal{L}_5, \mathcal{L}_6, \ldots$ generally involve all possible $SU(3)_c \times SU(2)_L \times U(1)_Y$ *symmetric* interaction terms of dimensions 5, 6, ... *They are the (non- renormalizable) remnants from the integration over the (presently) unobservable fields of the full theory* and if nonzero, provide small but crucial corrections for $\sqrt{s} \ll \Lambda$. A detailed classification of the terms allowed in $\mathcal{L}_5$ and $\mathcal{L}_6$ may be found in Refs.[7].

The new terms contribute to a variety of processes. The strength of each term is characterized by a dimensionless effective coupling parameter which is unknown at this level. A prediction of such couplings would require the detailed knowledge of the underlying theory. The most stringent experimental limits on the allowed strengths of such additional interaction terms come from rare decays and from high-energy scattering experiments, the subject of this paper.

Henceforth, I shall restrict the discussion to contact terms of the four-fermion type as contained in $\mathcal{L}_6$. They are relevant for a prominent class of $f_1 f_2 \to f_3 f_4$ (sub) processes to be studied at pp, $\bar{p}p$, $e^{\pm}p$ and e^+e^- colliders.

These contact terms may be visualized to arise predominantly from the exchange of virtual, new bosons X which, on the scale $\sqrt{s}$, are too heavy to propagate. Integrating these particles out amounts on the tree level to 'collapsing' the respective exchange diagrams into contact terms as depicted in Fig. 1.

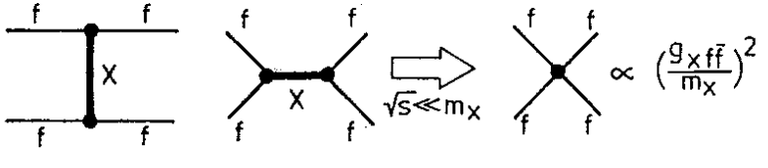

Figure 1: Heavy boson exchanges giving rise to four-fermion contact terms of effective strength $\propto (g_{Xf\bar{f}}/m_X)^2$.

By comparing the result with the expected effective strength $(g_{eff}/\Lambda)^2$ of a four-fermion contact term, one infers (c.f. Fig. 1)

$$g_{eff} = g_{Xf\bar{f}} \qquad \text{and} \qquad \Lambda \propto m_X. \tag{2}$$

[1] or more generally, field degrees of freedom which are unobservable at present energies

Of course, only the ratio g_{eff}/Λ can be determined experimentally. In the context of quark and lepton compositeness it has become customary to quote, nevertheless, experimental bounds for Λ by adopting the rather *ad hoc* normalization

$$g^2_{eff}/4\pi \equiv 1, \tag{3}$$

suggested only by a non-compulsive analogy to hadron physics. Since, in this paper I want to take a more general attitude as to the nature of the new physics involved, it is sensible to consider instead the scale

$$\Lambda^* = \Lambda/\sqrt{g^2_{eff}/4\pi}, \tag{4}$$

which is both directly measurable and such that

$$\Lambda^* = \Lambda \sim m_X \qquad \text{if} \qquad g^2_{eff} \simeq 4\pi. \tag{5}$$

However, if the contact term is e.g. due to the exchange of a distant Z' vector boson from some underlying GUT theory, say, one expects

$$g_{eff} \sim g_{weak} \simeq 0.64 \qquad \text{and then} \qquad \Lambda^* \simeq 5.5\Lambda \gg m_X \tag{6}$$

Let me illustrate the preceeding discussion with a very instructive example which I shall come back to also in Sect. 2.3. We consider $\sqrt{s} \ll m_{W,Z}$ such that the *weak* neutral current interactions due to Z exchange degenerate into the well known four-fermion *contact interactions*

$$\delta\mathcal{L}^{NC}_{eff} = -\frac{g^2_{weak}}{2m^2_W} J^{\nu}_{NC} J_{NC,\nu} \tag{7}$$

providing a small perturbation to pure QED processes. For example, by picking out of the product of weak neutral currents (7) the contact terms contributing to $e^+e^- \to \mu^+\mu^-$, one finds with $s^2 \equiv \sin^2\theta_W$

$$\begin{aligned}\delta\mathcal{L}^{\bar{e}e\bar{\mu}\mu}_{eff} &= \frac{(2-4s^2)^2}{8\Lambda^2_F}[\eta_{LL}(\bar{\mu}_L\gamma^{\nu}\mu_L)(\bar{e}_L\gamma_{\nu}e_L) + \eta_{LR}(\bar{\mu}_L\gamma^{\nu}\mu_L)(\bar{e}_R\gamma_{\nu}e_R) + \\ &+ \eta_{LR}(\bar{\mu}_R\gamma^{\nu}\mu_R)(\bar{e}_L\gamma_{\nu}e_L) + \eta_{RR}(\bar{\mu}_R\gamma^{\nu}\mu_R)(\bar{e}_R\gamma_{\nu}e_R)]\end{aligned} \tag{8}$$

where

$$\Lambda_F = \frac{2m_W}{g_{weak}} \simeq 246 \text{ GeV}, \tag{9}$$

and

$$\eta_{LL} \equiv -1;\ \eta_{LR} = \frac{s^2}{\frac{1}{2}-s^2};\ \eta_{RR} = -\left(\frac{s^2}{\frac{1}{2}-s^2}\right)^2, \tag{10}$$

i.e. the η's factorize, $\eta_{LL}\,\eta_{RR} = \eta^2_{LR}$, and are defined such as to satisfy

$$\max(|\eta|) = 1 \text{ and } |\eta| \leq 1. \tag{11}$$

By comparing Eq. (8) with the generic ansatz for contact terms (see Sect. 2.2) with strength $(g_{eff}/\Lambda)^2$ and identifying $g_{eff} = g_{weak} \simeq 0.64$, we find

$$\Lambda_{e\mu} = \frac{4\cos\theta_W}{2-4s^2} m_Z \simeq 0.29\ TeV \quad (12)$$

$$\Lambda^*{}_{e\mu} = \frac{4\sqrt{\pi}\Lambda_F}{2-4s^2} \simeq 1.6\ TeV. \quad (13)$$

Thus, in this example, Λ^* is directly related to the scale of electroweak symmetry breaking, Λ_F, defined in analogy to the scale of chiral flavor symmetry breaking, $f_\pi \simeq 95$ MeV, appearing in an effective lagrangian description of low energy hadron physics. In fact, Λ^* precisely corresponds to the energy, where (partial wave) unitarity would be violated if there was no physical Higgs boson in the Standard Model[8]! On the other hand, the scale Λ being much smaller than Λ^* due to the smallness of g_{weak}, is directly related to the mass of the 'new particle' Z^0 (as seen from low-energy QED).

After these attempts to illuminate contact interactions in general and the meaning of the associated scales Λ and Λ^*, let me now introduce the form of the contact interactions as relevant for future collider experiments.

2.2 Four-Fermion Contact Terms

Let me start by listing the various types of colliders together with the $f_1 f_2 \to f_3 f_4$ (sub) processes/contact terms of interest

Table 1:

collider	*four-fermion (sub) processes to be probed*		
e^+e^-	$e^+e^- \to l^+l^-$	$e^+e^- \to \bar{q}q$	–
$e^\pm p$	–	$e^\pm q \to e^\pm q$	–
pp, $\bar{p}p$	–	$\bar{q}q \to \bar{l}l$	$qq \to qq$, $\bar{q}q \to \bar{q}q$

We note the *unique*, complementary ability of e^+e^- and pp or $\bar{p}p$ colliders to provide information on possible four-fermion contact terms involving *only* leptons and *only* quarks, respectively. $e^\pm p$ colliders, instead, specialize on probing mixed $e-q$ interaction terms. These can be related via crossing or T invariance to mixed $e-q$ interaction terms at e^+e^- and pp or $\bar{p}p$ colliders. Clearly, the various scales Λ_{ll}, Λ_{lq} and Λ_{qq} may,*a priori*, be drastically different and, thus, the complementary information from different types of future colliders is vital for a *systematic, model independent* search programme.

Unfortunately, the most general ansatz for the contact terms involves (too) many unknown parameters. Therefore, a traditional restriction has been to include in experimental analyses or in simulations only those $SU(3)_c \times SU(2)_L \times U(1)_Y$ invariant four-fermion contact terms which conserve both helicity and flavor and correspond to color and isospin singlet exchanges,[2].

$$\delta\mathcal{L}^{4-f}_{eff} = \frac{4\pi}{\Lambda^{*\,2}} \sum_{i,j} \frac{1}{1+\delta_{ij}} [(\bar{f}^i_L\gamma^\mu f^i_L)(\bar{f}^j_L\gamma_\mu f^j_L)\eta^{ij}_{LL} + (\bar{f}^i_R\gamma^\mu f^i_R)(\bar{f}^j_R\gamma_\mu f^j_R)\eta^{ij}_{RR} +$$

[2]It is, indeed, hard to imagine that these terms -if present- are abnormally suppressed by (approximate) symmetries. In contrast, e.g. helicity changing contact terms are expected to involve extra suppression factors $\propto (m_{fermion}/\Lambda)^n$ due to an approximate chiral symmetry usually associated with light fermions

$$+ \ (\bar{f}^i_R\gamma^\mu f^i_R)(\bar{f}^j_L\gamma_\mu f^j_L)\eta^{ij}_{RL} + (\bar{f}^i_L\gamma^\mu f^i_L)(\bar{f}^j_R\gamma_\mu f^j_R)\eta^{ij}_{LR}]. \quad (14)$$

Here, i and j run through 'up' and 'down' quarks and leptons. The ignorance about the helicity structure in Eq. (14) is reflected in the unknown weights η with $|\eta| \leq 1$ and the largest $|\eta| \equiv 1$. $SU(2)_L$ invariance requires for 'up' and 'down' flavors

$$\eta^{ij}_{LL} = \eta_{LL};\ \eta^{ij}_{RL} = \eta^i_{RL};\ \eta^{ji}_{LR} = \eta^i_{LR}. \quad (15)$$

Moreover,

$$\eta^{ii}_{RL} = \eta^{ii}_{LR}. \quad (16)$$

Hence, at this level, one encounters, in principle,

- η_{LL}, η_{LR} and η_{RR} in case of $e^+e^- \to e^+e^-$,
- η_{LL}, η^i_{LR}, η^i_{RL} and η^i_{RR}; $i = u, d$ in case of $e^\pm q \to e^\pm q$,
- η_{LL}, η^i_{LR} and $\eta^{ij}_{RR} = \eta^{ji}_{RR}$; $i = u, d$ in case of $qq \to qq$ or $\bar{q}q \to \bar{q}q$.

It has become customary, to concentrate on standardized helicity configurations as summarized in Table 2. As to the four-quark contact terms, to my knowledge, only the first configuration, $LL_\pm$, in Table 2 has actually been taken into account in numerical analyses up to now.

Table 2: Standard helicity configurations for the contact terms

configuration	η_{LL}	η_{RR}	η_{RL}	η_{LR}
$LL_\pm$	±1	0	0	0
$RR_\pm$	0	±1	0	0
$RL_\pm$	0	0	±1	0
$LR_\pm$	0	0	0	±1
$VV_\pm$	±1	±1	±1	±1
$AA_\pm$	±1	±1	∓1	∓1
$WCS_\pm$	±1	∓1	0	0

In the bottom line of Table 2, I have included a peculiar choice of η values, corresponding to the so-called 'worst-case-study' (WCS) configuration[9,6,10,11,13]. It is motivated from the observation that often the dominant sensitivity to contact terms arises from their *interference* with the exchanged, *massless* vector bosons (γ, gluons) of the Standard Model. The WCS configuration in Table 2 just corresponds to combinations of η's such as to precisely cancel this interference term in the *unpolarized* cross section. As we shall see, however, the WCS configuration is only 'worst' in certain observables and processes, which illustrates already the importance of a systematic investigation at different colliders using a variety of observables (polarization!). It should also be mentioned that the WCS configuration is perhaps not naturally expected to occur in *elastic* (sub) processes, since there for exchanges of new, heavy vector particles, η_{RR} and η_{LL} represent sums of couplings squared and, therefore, cannot have different signs.

In a new analysis for future pp colliders in Sect. 3.3, I shall also consider the effects from contact terms due to the most general helicity conserving, $SU(3)_c \times SU(2)_L \times U(1)_Y$ invariant contact interaction among up and down quarks[4,5]. This amounts to including four additional terms in Eq. (14)

$$\begin{aligned}\delta\mathcal{L}'_{eff} &= \delta\mathcal{L}^{4-f}_{eff} + \\ &+ \frac{4\pi}{\Lambda^{\star\,2}}\{\eta^1_{LL}(\bar{q}_L\gamma^\mu\frac{\tau^a}{2}q_L)(\bar{q}_L\gamma_\mu\frac{\tau^a}{2}q_L) + \eta^{'ud}_{RR}(\bar{u}_R\gamma^\mu d_R)(\bar{d}_R\gamma_\mu u_R) + \\ &+ \eta^{8u}_{LR}(\bar{q}_L\gamma^\mu\frac{\lambda^A}{2}q_L)(\bar{u}_R\gamma_\mu\frac{\lambda^A}{2}u_R) + \eta^{8d}_{LR}(\bar{q}_L\gamma^\mu\frac{\lambda^A}{2}q_L)(\bar{d}_L\gamma_\mu\frac{\lambda^A}{2}d_R)\} \qquad (17)\end{aligned}$$

with

$$q_L = (u,d)^t_L, \qquad (18)$$

and the three $SU(2)_L$ and eight $SU(3)_c$ generators $\tau^a/2$ and $\lambda^A/2$, respectively. Thus, there are 10 independent four-quark contact terms of strengths

$$\eta_{LL},\ \eta^1_{LL},\ \eta^u_{LR},\ \eta^d_{LR},\ \eta^{8u}_{LR},\ \eta^{8d}_{LR},\ \eta^{uu}_{RR},\ \eta^{ud}_{RR},\ \eta^{'ud}_{RR},\ \eta^{dd}_{RR}, \qquad (19)$$

the contributions of which to the various $qq \to qq$ cross sections is found after a lengthy calculation[12]

$$\frac{d\hat{\sigma}}{d\hat{t}}(ij \to i'j') = \frac{\pi}{\hat{s}^2}|A(ij \to i'j')|^2, \qquad (20)$$

with $(i = u, d)$

$$\begin{aligned}|A(ii \to ii)|^2 &= \alpha_s(Q^2)^2\{\frac{4}{9}(\frac{\hat{s}^2+\hat{u}^2}{\hat{t}^2} + \frac{\hat{s}^2+\hat{t}^2}{\hat{u}^2} - \frac{2}{3}\frac{\hat{s}^2}{\hat{t}\hat{u}}) + \\ &+ \frac{8}{9}(\frac{\hat{s}^2}{\hat{t}} + \frac{\hat{s}^2}{\hat{u}})(\mu_{LL} + \mu^{ii}_{RR}) + \frac{8}{9}(\frac{\hat{u}^2}{\hat{t}} + \frac{\hat{t}^2}{\hat{u}})\mu^{8i}_{LR} + \\ &+ \frac{8}{3}\hat{s}^2(\mu^2_{LL} + (\mu^{ii}_{RR})^2) + (\hat{u}^2+\hat{t}^2)(\frac{4}{9}(\mu^{8i}_{LR})^2 + 2(\mu^i_{LR})^2)\}, \qquad (21)\end{aligned}$$

and

$$\begin{aligned}|A(ud \to ud)|^2 &= \alpha_s(Q^2)^2\{\frac{4}{9}\frac{\hat{s}^2+\hat{u}^2}{\hat{t}^2} - \frac{8}{9}\frac{\hat{s}^2}{\hat{t}}(\mu^1_{LL} + \mu^{'ud}_{RR}) + \frac{4}{9}\frac{\hat{u}^2}{\hat{t}}(\mu^{8u}_{LR} - \mu^{8d}_{LR}) + \\ &+ \hat{s}^2[\mu^2_{LL} + \frac{8}{3}(\mu^1_{LL})^2 - \frac{8}{3}\mu_{LL}\mu^1_{LL} + (\mu^{ud}_{RR})^2 + (\mu^{'ud}_{RR})^2 - \frac{2}{3}\mu^{ud}_{RR}\mu^{'ud}_{RR}] + \\ &+ \hat{u}^2[(\mu^u_{LR})^2 + (\mu^d_{LR})^2 + \frac{2}{9}((\mu^{8u}_{LR})^2 + (\mu^{8d}_{LR})^2)]\}, \qquad (22)\end{aligned}$$

with the abreviations

$$\mu = \frac{\eta}{\alpha_s(Q^2)\Lambda^{\star\,2}}. \qquad (23)$$

All remaining cross sections are obtained from Eqs. (21, 22) by $\hat{s} \leftrightarrow \hat{u}$ and $\hat{s} \leftrightarrow \hat{t}$ crossing. First of all, let me point out that the contributions from the square of the contact terms to

the $uu \to uu$ and $ud \to ud$ cross sections as quoted for the special case LL in Refs. [3,4,5], are actually incorrect[3]. By using the wrong form, one obtains significantly lower values of $\Lambda^\star$ in pp collisions.

The generalized ansatz, Eqs. (21, 22), exhibits the following features in comparison with the usual LL form.

- Apparently, seven out of the ten helicity couplings occur in interference terms which will to some extent enhance the sensitivity to these parameters. The cross section for $ud \to ud$ (and $u\bar{d} \to u\bar{d}, u\bar{u} \to d\bar{d}, \ldots$) now may have an interference term, too.
- For the case of all η's contributing equally with equal signs (VV_+), one expects a significant improvement[6] in the 'reach' (c.f. Sect. 3.3)

$$\Lambda^\star{}_{VV} \approx 1.5\Lambda^\star{}_{LL}, \qquad (24)$$

as compared to previous studies of pp and $\bar{p}p$ collisions, where only the $LL_\pm$ configurations were considered.

2.3 Analytical Insight

Usually, in real experiments or simulations, the 'reach' $\Lambda^\star$ for contact interactions is obtained via numerical fits. They certainly provide the most precise results. However, notably in case of simulations for future colliders, the operation of which will start years from now, it seems appropriate to trade some precision for analytical insight into the crucial dependences of $\Lambda^\star$ on energy $\sqrt{s}$, integrated luminosity $\int Ldt$ and the process in question.

Therefore, in this Section, I shall discuss a simple scaling law and semi quantitative analytical expressions[6,9,10] for $\Lambda^\star$. Such results are particularly useful for quickly estimating and comparing the potential 'sensitivity' of future colliders to new physics. A comparison with 'state of the art' numerical simulations is deferred to Sect. 3.

Let me begin with the scaling law.

In our problem, there are, in general, four relevant *dimensionful* quantities

$$\Lambda^\star\ ,\ \sqrt{s},\ \int Ldt \text{ and } \Lambda_{QCD}. \qquad (25)$$

The QCD scale Λ_{QCD} enters, in principle, to characterize the effects from QCD scaling violations. However, even in case of hadron colliders where the cross sections are

$$\hat{\sigma} \propto \alpha_s(Q^2/\Lambda^2_{QCD})^2, \qquad (26)$$

and hadronic structure functions enter, the QCD scaling violations turn out to largely cancel in expressions for the bounds on $\Lambda^\star$, if extracted from suitable observables.

A bound on $\Lambda^\star$ is defined via a 'confidence' criterion, like a χ^2. The χ^2-function is a complicated expression, involving summation over (real or simulated) data, errors and theory depending on $\Lambda^\star$. Nevertheless, the χ^2 is *dimensionless* and a typical 95% confidence level criterion

[3] I thank Estia Eichten for a communication on this point.

$$\Delta\chi^2 = 4, \tag{27}$$

then should depend only on dimensionless *ratios* of our dimensionful quantities (25), while any additional dimensionless (kinematical) variables are summed (integrated) over. Thus, ignoring effects from Λ_{QCD}, there are only two independent ratios, $\Lambda^* / \sqrt{s}$ and $\int Ldt/s$, say, and the criterion (27) implicitely defines

$$\frac{\Lambda^*{}_{95\%CL}}{\sqrt{s}} = f(\frac{\int Ldt}{s}). \tag{28}$$

Clearly, the functional dependence in this simple scaling law depends on the details of the specific criterion applied (like kinematical cuts, systematical errors, etc.), the observable from which Λ^* is extracted and the process under consideration[4].

In Sect. 3.3, we shall confront Eq. (28) to realistic numerical simulations, e.g. the complex case of pp collisions and illustrate its validity and usefulness.

At this point, we may draw two conclusions:

- Future colliders satisfying $\int Ldt/s \approx const.$ (which is advisable for reasons of rate), give

$$\Lambda^* \propto \sqrt{s}. \tag{29}$$

- Knowing the function $f(\int Ldt/s)$ in Eq. (28) for a range of $\int Ldt$ and/or s values either from present experiments or existing simulations, allows an immediate evaluation of Λ^* for any different s but fixed $\int Ldt/s$.

What can we say about the functional form entering Eq. (28)?

Let us concentrate on the c.m. angular distribution $d\hat{\sigma}/dz$, $z = cos\theta$, of a four-fermion (sub) process with total c.m. energy $\sqrt{\hat{s}}$. Of course, for $e^+e^- \to \bar{f}f$, $\hat{s} = s$, $\hat{\sigma} = \sigma$.

After adding the contact terms to the Standard Model (SM) amplitudes, the cross section may be written as

$$\frac{d\hat{\sigma}}{dz}_{|\Lambda^*} = \frac{d\hat{\sigma}}{dz}_{|SM} + 2\sqrt{\frac{d\hat{\sigma}}{dz}_{|SM}} \frac{\sqrt{\hat{s}}}{\Lambda^{*\,2}} \{\eta h_1(z) + h_2(z)(\frac{\eta\sqrt{\hat{s}}}{\Lambda^*})^2\} \tag{30}$$

The first term in the bracket is due to an *interference* of the contact term with the SM amplitude and often dominates (typically in e^+e^- collisions). The second term corresponds to the square of the contact term. It gains increasing importance for very high energy pp or $\bar{p}p$ collisions. The parameter η is to characterize the helicity configuration of the contact term, $|\eta| \leq 1$, as in Eq. (14). Moreover, one typically finds

$$\int_{-1}^{+1} dz h_1^2(z) = O(1). \tag{31}$$

For $e^+e^- \to \bar{f}f$, the situation is then quite simple.

Ignoring systematical errors and keeping only the interference term in (30), we compare by means of the χ^2-function the relative deviation

[4]More involved criteria or extraction of Λ^* from certain observables (c.f. Ref. [4]), in fact, invalidate the simple scaling (28), typically through an additional dependence on $\sqrt{s}/\Lambda_{QCD}$.

$$\Delta \equiv \left(\frac{\frac{d\sigma}{dz}_{|\Lambda^*}}{\frac{d\sigma}{dz}_{|SM}} - 1 \right) \simeq 2 \frac{h_1(z)}{\sqrt{\frac{d\sigma}{dz}_{|SM}}} \eta \frac{\sqrt{s}}{\Lambda^{*\,2}}, \tag{32}$$

with the statistical errors

$$\epsilon_\Delta = \frac{1}{\sqrt{dN(z)}} = \frac{1}{\sqrt{\frac{d\sigma}{dz}_{|SM} \Delta z \int Ldt}}, \tag{33}$$

where $dN(z)$ is the number of events falling between z and $z + \Delta z$.

The 95% CL bound on Λ^* is obtained from

$$\begin{aligned} \Delta\chi^2 &= \sum_{z_i} \frac{\Delta^2}{\epsilon_\Delta^2} \qquad (= 4) \\ &= \underbrace{[\sum_{z_i} \Delta z h_1^2(z_i)]}_{\approx 1 \text{from (31)}} \frac{4\eta^2 s \int Ldt}{\Lambda^{*\,4}}. \end{aligned} \tag{34}$$

Solving for $\Lambda^* / \sqrt{s}$, one finds the simple formula[9,6,10,11]

$$\frac{\Lambda^*}{\sqrt{s}} \simeq (4\eta^2/\Delta\chi^2)^{1/4} \left(\frac{\int Ldt}{s} \right)^{1/4}, \tag{35}$$

of course in agreement with the more general scaling form (28).

We conclude from Eq. (35)

- Since Λ^* increases only with the fourth root of $\int Ldt$, 'patience' does not really pay off!
- The numerical coefficient $(4\eta^2/\Delta\chi^2)^{1/4}$ is typically $O(1)$ and - due to the fourth root involved - only weakly dependent on the χ^2 criterion, a restricted angular acceptance or the details of the Standard Model amplitudes.

For a first, pedagogical application of formula (35), let us return to our illustration in terms of the four-fermion contact term limit of the weak interactions from Sect. 2.1.

We may use Eq. (35) to immediately quote the luminosity needed in an e^+e^- machine to observe effects from the *weak* scale $\Lambda^*{}_{weak} \simeq 1.6$ TeV, Eq. (13), in $e^+e^- \to \mu^+\mu^-$, say. Eq. (31) reads in this case

$$\int_{-1}^{+1} dz h_1^2(z) = \frac{2\pi}{(2 - 4\sin^2\theta_W)^4} \int_{-1}^{+1} dz \frac{z^2}{1+z^2} = \frac{\pi(4-\pi)}{(2-4\sin^2\theta_W)^4} \simeq 2.0, \tag{36}$$

such that from Eq. (35)

$$(\int Ldt)_{95\%CL} \simeq \left(\frac{\pi}{4-\pi} \right) \frac{(4\Lambda_F)^4}{s}. \tag{37}$$

In Fig. 2, the luminosity needed according to Eq. (37) is displayed as a function of $\sqrt{s}$ together with the luminosity taken by HRS/ PEP[14], JADE/ PETRA [15] and AMY/ TRISTAN [16]. While at the lower energies rather high statistics experiments are needed to spot

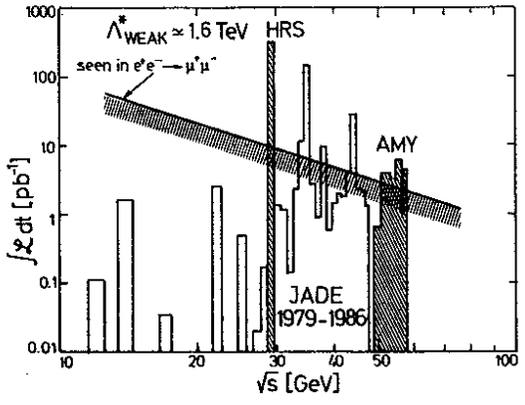

Figure 2: Spotting effects from *weak* contact terms in $e^+e^- \to \mu^+\mu^-$. The necessary luminosity according to Eq. (37) is displayed along with the one taken by representative PEP, PETRA and TRISTAN experiments.

the *weak* contact terms, statistics is no problem for TRISTAN due to the higher energy available.

For *ep* and *pp* or $\bar{p}p$ collisions it becomes an increasingly complex task to derive useful approximations for the functional form appearing in the scaling law (28). The complications come, of course, from the nucleon structure functions and for *pp* and $\bar{p}p$ collisions, in particular, from the gg and qg subprocesses which dominate over the four-quark subprocesses in a wide range of phase space.

Nevertheless, let me make a few 'analytical' remarks on the complex case of *pp* and $\bar{p}p$ collisions.

As will be argued in more detail in Sect. 3.3, a very suitable observable for extracting bounds on Λ^* is the 2-jet angular distribution, normalized to the integrated 2-jet cross section[17,18]. In order to enhance the signal from possible contact interactions relative to the qg and gg subprocesses, one has to consider sufficiently large 2-jet masses $m_{2-jet} \equiv \sqrt{\hat{s}}$

$$\sqrt{\tau} = m_{2-jet}/\sqrt{s} \geq 0.25, \text{ say,} \tag{38}$$

as apparent from Fig. 3.

In this domain of $\hat{s}$ the square of the contact term becomes increasingly important. By repeating the same steps as above, however, taking into account in Eq. (30)the square of the contact term only, one arrives at a similar formula as (35) with the power 1/4 replaced by 1/8.

In conclusion, we may expect in *pp* or $\bar{p}p$ collisions a behaviour like in (35), but with a power around 1/6, say.

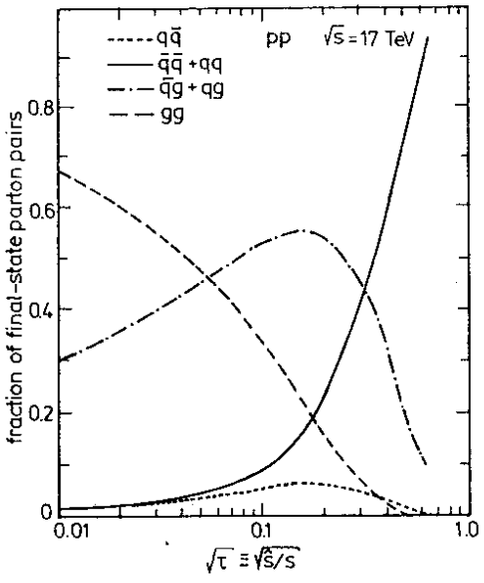

Figure 3: Fraction of final-state parton pairs versus $\sqrt{\tau}$ in case of the LHC, from Ref. [18].

3 Selected Results From Simulations

3.1 e^+e^- Collisions - A Clean Reference Case

A systematic (numerical) study of the 'reach' Λ^* for possible new contact interactions at e^+e^- colliders has been performed in Ref. [10,11,13]. Let me summarize some essential aspects and also compare the numerical results for Λ^* with the simple analytical formula (35), as derived in Sect. 2.3. The reactions under consideration were $e^+e^- \to e^+e^-, \mu^+\mu^-$. The analysis is distinguished by the following features

- A large energy range was considered, from PETRA/ PEP energies at the lower end, via the Z^0 peak (LEP/ SLC) and LEP II, up to the TeV regime of a potential future linear e^+e^- collider (CLIC).
- Realistic assumptions on the expected luminosities and detector performances were made.
- Besides the expected statistical errors, a systematic error of 3% coming from the error on the luminosity measurement was taken into account.
- The bounds for Λ^* resulting from simulated 'data' were shown to agree with the actual experimental limits from PETRA and PEP within the range allowed by the various experimental measurements.

- The impact of *longitudinal* and transverse beam polarization was studied in detail (c.f. Sect. 3.2).
- The question of radiative corrections was considered.

Fig. 4 illustrates the quality of expected data and the effects of contact interactions in representative helicity configurations (c.f. Table 2) for LEP II with $\int Ldt = 500\ pb^{-1}$ and $\Lambda^* = 5\ TeV$. Plotted is the deviation

$$\Delta \equiv \left(\frac{d\sigma}{dz}_{|\Lambda^*} / \frac{d\sigma}{dz}_{|SM} - 1 \right), \tag{39}$$

versus $z = cos\theta$.

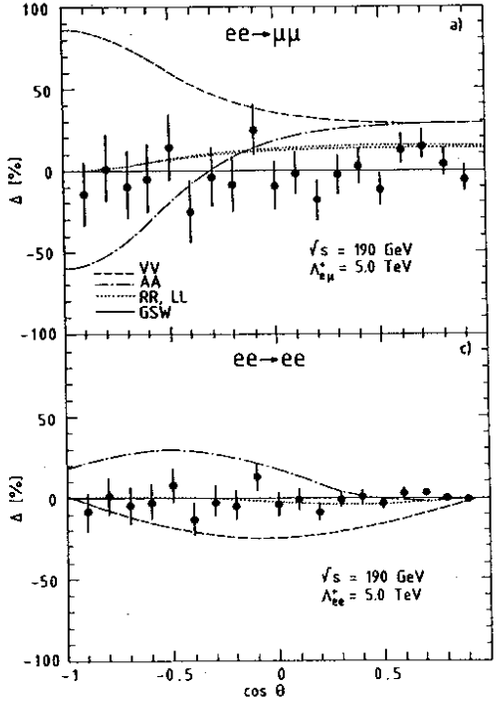

Figure 4: Quality of expected data (LEP II) and the effect of contact terms on $d\sigma/dcos\theta$ for $e^+e^- \to \mu^+\mu^-$ (a), and $e^+e^- \to e^+e^-$ (c). Δ is the relative deviation from the Standard Model cross section.

The analytic formula for Λ^* , Eq. (35), suggests to define a *reduced* 'reach' Λ_{red}, by dividing out the machine dependent 'patience' factor $(\int Ldt/s)^{1/4}$,

$$\Lambda_{red} = \Lambda^*_{\ 95\%CL} \left[\frac{s}{(190\ GeV)^2} \frac{500\ pb^{-1}}{\int Ldt} \right]^{1/4} \equiv \Lambda^*_{\ LEP\ II}. \tag{40}$$

In Eq. (40), I have normalized to the conditions expected at LEP II within a few years of operation. Moreover, it so happens that $\Lambda_{red} = \Lambda^*$ if $\int Ldt \approx 65\ pb^{-1}$, $100\ pb^{-1}$ and $15\ fb^{-1}$ for PETRA (47 GeV), LEP and CLIC (1 TeV), respectively, which allows a uniform comparison of the 'reach' for these e^+e^- colliders.

Fig. 5 shows the results for Λ_{red} from the numerical simulation as a function of $\sqrt{s}$ from 30 GeV to 5 TeV. The solid lines correspond to the two extreme helicity configurations VV and WCS, as well as to LL. Indeed, apart from the Z^0 pole, Λ_{red} shows to very good approximation a $\sqrt{s}$ behaviour, as expected from Eqs. (35, 40).

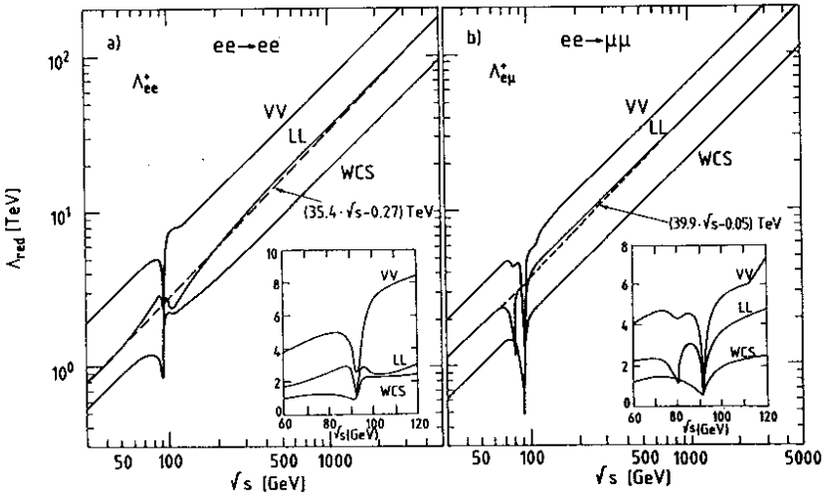

Figure 5: The reduced 'reach', Λ_{red} of Eq. (40) for e^+e^- colliders as a function of $\sqrt{s}$ behaving as expected $\propto \sqrt{s}$ (dashed line). The most favorable (VV), the most insensitive (WCS) and the LL helicity configurations are displayed. The inserts magnify the 'insensitive' region around the Z^0 peak.

Energy is, therefore, the determining factor for the 'reach'. On the Z^0 pole, the Standard Model amplitude is imaginary and, thus, cannot interfere with the real contact term. Since in e^+e^- collisions the interference term is crucial, the sensitivity is very bad right on the Z^0!(see also the inserts in Fig. 5). The general importance of the interference term in e^+e^- collisions is also made obvious by the strong suppression of the WCS configuration (c.f. Sect. 2.3).

3.2 Impact of Longitudinal Polarization at HERA and LEP

The interest in polarized beams for the study of contact terms arises mainly for the following reasons

- By means of longitudinal beam polarization one may hope to increase the sensitivity to particular helicity couplings, where unpolarized data are comparatively insensitive (e.g. WCS, LL, RR in e^+e^-).

- Once a signal has been found in unpolarized data, longitudinal polarization will be crucial in disentangling the various helicity couplings.

The impact of polarization on contact interactions has been extensively studied for $e^{\pm}p$ collisions (HERA, LHC-ep) in Refs. [19,20,21] and for e^+e^- collisions in Ref. [10,11].

One may hope that at a later stage of operation longitudinally polarized e^- and e^+ beams will be made available at HERA, such that the differential cross sections

$$d^2\sigma(e^{\mp}_{L,R}p \to e^{\mp}_{L,R}X)/dxdQ^2 \tag{41}$$

may be studied experimentally.

In Fig. 6 the bounds for $\Lambda^*{}_{eq}$ as extracted from simulated 'data' [20] for these four cross sections are displayed for HERA with $\sqrt{s} = 314$ GeV, $\int Ldt = 100\ pb^{-1}$ and $P = 80\%$. The ability of polarized cross-section measurements to filter out a particular chirality component in the contact terms is nicely apparent in this type of plot. The LL (RR) couplings are most sensitive to e^-_L(e^-_R) beams and least sensitive to e^+_L(e^+_R) beams, to which the RL(LR) couplings, in turn, are most sensitive.

Fig. 7 illustrates an analogous pattern for the case of $e^+e^- \to e^+e^-$ (LEP II). Here, the bounds for $\Lambda^*{}_{ee}$ corresponding to LL_+, RR_+, VV_+, and WCS_+ couplings from the unpolarized $d\sigma/dcos\theta$ are compared to those from $d\sigma^{\pm 50\%}/dcos\theta$ and from the left-right asymmetry $A_{LR}^{\pm 50\%}$ with +50% and -50% longitudinal beam polarization, respectively. While the sensitivity to WCS (VV) was worst (best) in $d\sigma^{unpol.}/dcos\theta$, it is best (worst) in A_{LR}!

These two examples clearly underlign the virtues of longitudinal beam polarization in the context of contact interactions.

3.3 A New Analysis for pp and $\bar{p}p$ Collisions

Several years ago, a detailed, well known study of the 'reach' Λ^* at future pp and $\bar{p}p$ colliders in the multi-TeV range has been performed[4] (EHLQ). The values for $\Lambda^*{}_{qq}$ were extracted from the inclusive jet production cross section, $d^2\sigma/dp_\perp dy_{|y=0}$, at high $p_\perp$, e.g. with the result

$$\Lambda^*{}_{qq} = O(20\ TeV) \tag{42}$$

for the SSC(40 TeV) with $\int Ldt = 10^4\ pb^{-1}$. Only the $LL_\pm$ helicity couplings were considered in this work.

Experimentally, the inclusive jet cross section at high $p_\perp$ is known to be subject to considerable normalization uncertainties and other systematical errors. Given the huge range of extrapolation, the inherent theoretical uncertainties are, indeed, surprisingly small, as pointed out in[4]. Nevertheless, the analysis of $d^2\sigma/dp_\perp dy_{|y=0}$ requires the detailed knowledge of *both* the x and Q^2 dependences of the nucleon structure functions, and the predictions do vary from one parametrization to another in the $p_\perp/\sqrt{s}$ range of interest. In view of these reasons a relatively 'coarse' confidence criterion for extracting Λ^* was applied in the EHLQ analysis, leading, in turn, to somewhat low values of Λ^* .

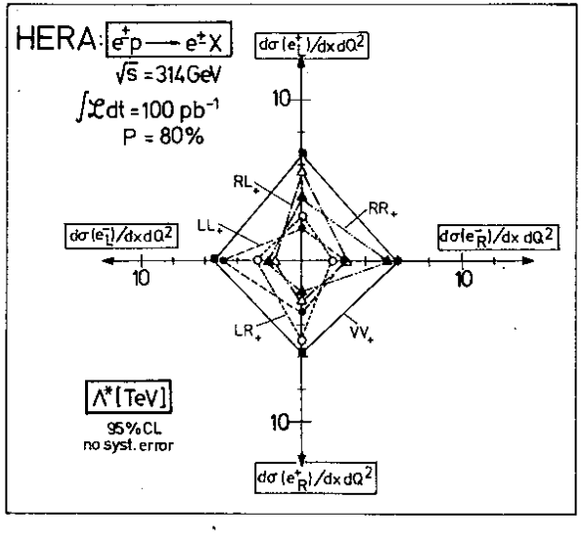

Figure 6: Λ^* extracted from simulated HERA 'data'. The ability of polarized cross-section measurements to filter out a particular chirality component in the contact terms is nicely apparent.

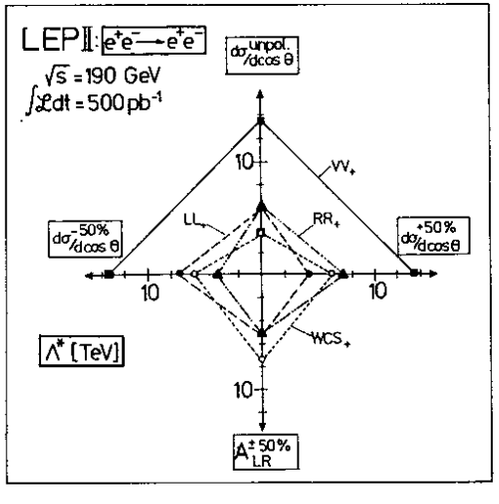

Figure 7: Impact of longitudinal beam polarization at LEP II. While the sensitivity to the WCS (VV) helicity configuration was worst (best) in $d\sigma^{unpol.}/dcos\theta$, it is best (worst) in the left-right asymmetry A_{LR}!

On the other hand, actual *experimental* studies of the normalized two-jet angular distribution for high 2-jet masses at the $S\bar{p}pS$ indicate[17,22] that this observable is best suited for a reliable extraction of bounds on Λ^* . Experimentally, the systematical errors are fairly small, essentially, because the c.m. scattering angle depends primarily on the measurement of jet directions which can be well determined in a large calorimetric detector. The (normalized) two-jet angular distribution has the advantage that in the limit of vanishing QCD scaling violations it is virtually *independent* of the structure functions, due to an approximate factorization into an effective structure function times an angular distribution corresponding to a single effective subprocess.[23]

Let me summarize next the results from a new analysis of the 'reach' Λ^* , I have performed for pp (and $\bar{p}p$) colliders. For the reasons mentioned above, it is based on (simulated) data for the normalized 2-jet angular distribution

$$\frac{1}{\sigma_{2-jet}(\chi<19)}\frac{d\sigma^{2-jet}}{d\chi} \quad \text{for} \quad \sqrt{\tau_0}\le\sqrt{\tau}\equiv\frac{m_{2-jet}}{\sqrt{s}}\le\sqrt{\tau_1}. \tag{43}$$

Here, χ is the popular angular variable[23,17]

$$\chi=\frac{1+\cos\theta}{1-\cos\theta}, \tag{44}$$

in terms of which the prominent forward (backward) peaks from the exchange of vector particles

$$\frac{d\sigma}{d\cos\theta}\propto\frac{1}{(1-\cos\theta)^2}, \tag{45}$$

are transformed into

$$\frac{d\sigma}{d\chi}\simeq const., \tag{46}$$

such that Eq. (46) represents a good approximation to the angular distribution from the lowest order subprocesses.

Let me point out some important features of the present analysis

1. A large energy range was considered, from $S\bar{p}pS$ energies, via the LHC and SSC regimes, up to a potential 200 TeV super collider (ELOISATRON), to which this workshop is devoted.

2. The kinematical cuts are directly adapted from the experience gained by actual $S\bar{p}pS$ experiments. In particular[17]

   (a) $1\le\chi\le 19$ is used which corresponds to $0\le\cos\theta_{2-jet}\le 0.9$.

   (b) The cross section (43) is integrated over scaled two-jet masses in the range $\sqrt{\tau_0}\le\sqrt{\tau}\le\sqrt{\tau_1}=0.45$ with

   $$\sqrt{\tau_0}=0.15 \text{ to } 0.35,$$

   depending on $\int Ldt$, such that at least $O(50)$ events are left.

3. A systematic error of 15% is included throughout.

4. EHLQ structure functions, set 1 with $\Lambda_{QCD}=200$ MeV, are used and $Q^2=p_\perp^2$ is taken to incorporate QCD scaling violations in the structure functions and via $\alpha_s(Q^2)$.

5. The present analysis is very close in spirit to the one performed[10] for the $e^+e^-\to\bar{f}f$ angular distribution, thus allowing for a direct comparison of the 'reach' at e^+e^- and pp colliders. In particular, the same 95 % CL criterion is used.

6. The most general and correct (c.f. Sect. 2.2) ansatz (17 , 21, 22) for the four-quark contact terms was incorporated.

Fig. 8 illustrates simulated 'data' for the normalized 2-jet angular distribution (43) as a function of χ according to the Standard Model at the $S\bar{p}pS$ and the SSC(40 TeV) with $\int Ldt=10^4\,pb^{-1}$. The error bars shown include a 15% systematical error besides the statistical one[5]. The 2-jet masses are integrated over in the range corresponding to $0.35\le\sqrt{\tau}\le 0.45$. Also shown in Fig. 8 are the effects of LL_- contact terms (here corresponding to $\Delta\chi^2\simeq 11$). At 95% CL ($\Delta\chi^2=4$) I find

$$\Lambda^*\simeq 392 \text{ GeV} \tag{47}$$

for the $S\bar{p}pS$ with $\sqrt{s}=630$ GeV and $\int Ldt=260\ nb^{-1}$, in good agreement with actual experimental results[17,22].

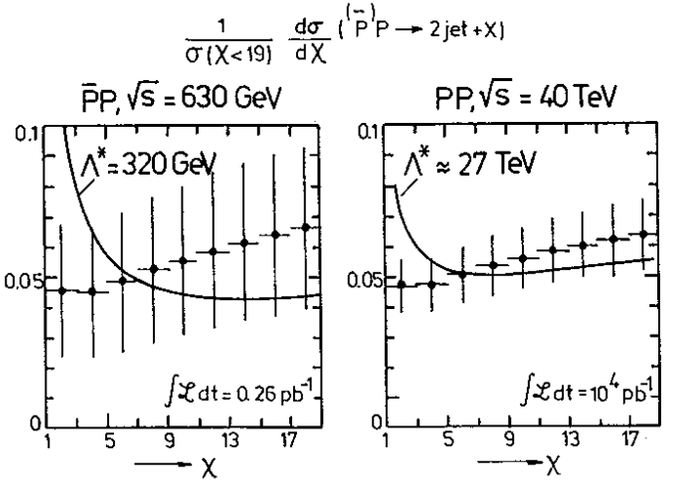

Figure 8: Simulated 'data' according to the Standard Model and effects of contact terms at the $S\bar{p}pS$ and the SSC.

[5] While my computer program was checked against a number of different distributions (including absolute normalization) from different authors, there remains a 'mystifying' disagreement with [17] *both* as to the size of the error bars (computed here from the SM cross sections and given $\int Ldt$) and the effect of the contact terms. Amazingly, the end result (47) *agrees*! The normalized χ distribution also agrees with the one shown in[17].

Fig. 9 displays the dependence of $\sigma_{2-jet}(\chi < 19)$ and Λ^* as extracted from (43) on different parametrizations for the nucleon structure functions[24]. While $\sigma_{2-jet}(\chi < 19)$ varies by as much as a factor of 1.5 both for the $S\bar{p}pS$ and the SSC (40 TeV), Λ^* is very insensitive, indeed, which underligns the reliability of the method used.

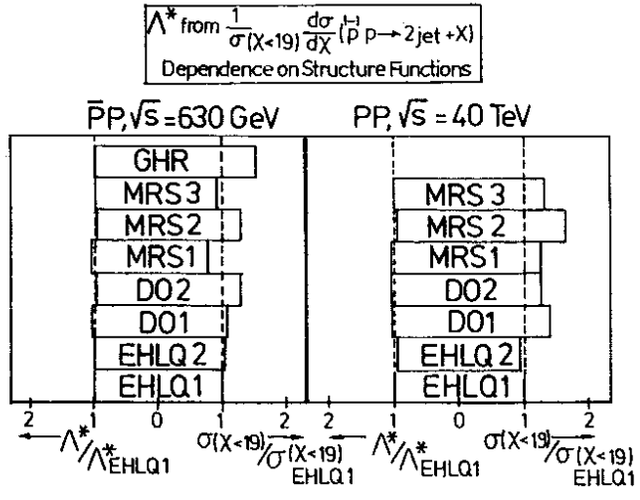

Figure 9: Dependence of $\sigma_{2-jet}(\chi < 19)$ and Λ^* on different parametrizations of the nucleon structure functions[24]. Unlike σ_{2-jet}, Λ^* is quite insensitive which underligns the reliability of the method used to extract Λ^*.

The next issue concerns the choice of the starting value $\sqrt{\tau_0}$ in the integration of (43) over the scaled 2-jet masses.

If $\sqrt{\tau_0}$ is decreased, the statistical errors decrease due to a strong rise of σ_{2-jet}, while the systematical errors, of course, remain unaffected. The importance of the contact terms, however, decreases due to the increasing importance of the qg subprocess. If $\sqrt{\tau_0}$ is increased, the importance of the contact terms in the 4-quark cross sections increases, but, eventually, one runs out of statistics!

This is illustrated in Fig. 10a, where $\Lambda^*{}_{95\%\ CL}$ has been determined as a function of $\sqrt{\tau_0}$ for the SSC and the ELOISATRON with $\int Ldt = 10^4\ pb^{-1}$ and $10^3\ pb^{-1}$. The larger luminosities, of course, admit larger $\sqrt{\tau_0}$ values.

Fig. 10b demonstrates that to good approximation the $\sqrt{\tau_0}$ dependence of Λ^* *factorizes* and indicates already that the scaling law (28) holds well for pp collisions. Fig. 10b contains the same points as Fig. 10a. A good parametrization is

$$\frac{\Lambda^*}{\sqrt{s}} \simeq g(\sqrt{\tau_0}, \sqrt{\tau_1}) \left(\frac{\int Ldt}{s}\right)^{0.155} \tag{48}$$

with $\sqrt{\tau_0}$ optimally chosen in the range 0.15 to 0.35, depending on $\int Ldt$.

Figs. 11, 12 contain the main results of this analysis.

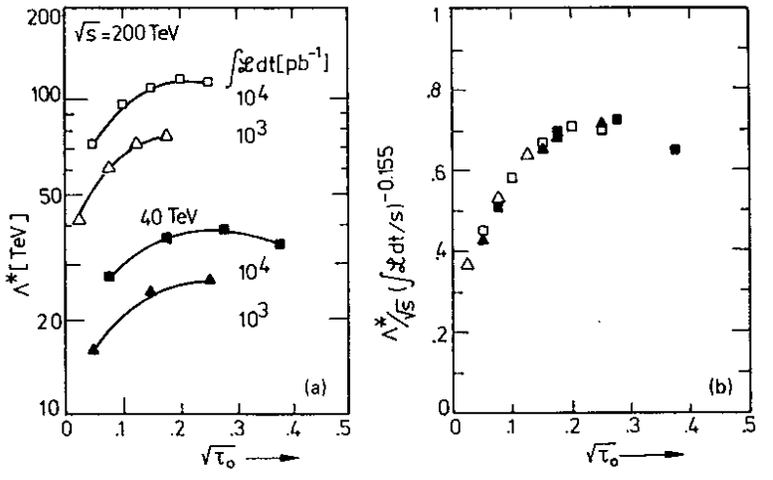

Figure 10: (a) Λ^* as a function of $\sqrt{\tau_0}$; (b) the same points replotted, demonstrating a factorization of the τ_0 dependence.

Fig. 11a shows the 95% CL bounds on Λ^* for pp colliders as a function of $\sqrt{s}$ for a large range of $\int Ldt$. The LL_- helicity configuration is displayed. For the ELOISATRON one finds, for instance,

$$\Lambda^*{}_{qq}(200\ TeV) \simeq O(100\ TeV), \tag{49}$$

for $\int Ldt = 10^4\ pb^{-1}$.

Fig. 11b contains the same points as Fig. 11a, however, this time $\Lambda^*/\sqrt{s}$ is plotted versus $\int Ldt/s$.

All points fall nicely on a *universal* curve and the very good validity of the scaling law (28) becomes apparent! The functional form is approximately a power law[25]

$$\frac{\Lambda^*}{\sqrt{s}} \propto \left(\frac{\int Ldt}{s}\right)^{\gamma}, \tag{50}$$

where

$$\gamma \simeq 1/6, \tag{51}$$

ranging as expected from Sect. 2.3, in between $\gamma = 1/4$ (interference term only) and $\gamma = 1/8$ (square of contact term only). The flattening of the universal curve in Fig. 11b for the larger $\int Ldt/s$ values, i.e. larger event numbers, is an effect due to the systematical error which begins to win over the decreasing statistical one there. Nevertheless, the scaling law holds irrespective of systematical errors. There is also no trace of QCD scaling violations visible from Fig. 11b.

The usefulness of the scaling law should be obvious, given the substantial computing effort necessary in pp collisions to extract values of Λ^*. Amazingly, while the scaling curve in Fig. 11b was made up from pp points in the range $\sqrt{s} \geq 17$ TeV and $\int Ldt \geq 10^2\ pb^{-1}$,

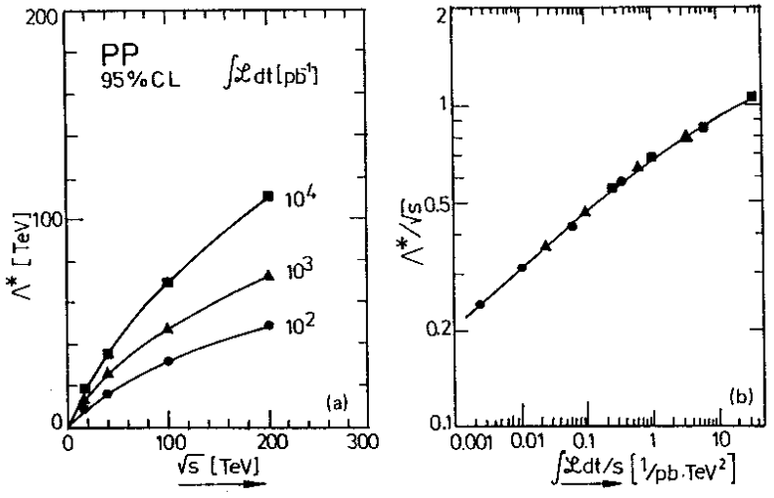

Figure 11: (a) Λ^* at 95% CL versus $\sqrt{s}$ for LL_- helicity couplings and pp colliders with different values of $\int Ldt$; (b) same points replottet, demonstrating the validity of the scaling law (28).

even the $\bar{p}p$ result (47) for the $S\bar{p}pS$ with $\sqrt{s} = 0.63$ TeV and $\int Ldt = 0.26\ pb^{-1}$, fits right onto the same curve!

Let me point out again, however, that the validity of the scaling law refers to a given 'confidence' criterion and a particular (suitable) observable from which Λ^* is extracted. For instance, it does not hold as well for the Λ^* values from the EHLQ analysis[4].

Finally, in Fig. 12, Λ^* corresponding to different helicity configurations is displayed versus $\sqrt{s}$ for pp collisions. At high energies, the most sensitive coupling is VV_- i.e. all 10 η's in Eq. (19) being equal to -1, and the least sensitive one is LL_+. Indeed, one finds roughly

$$\Lambda^*_{\ VV_-} \simeq 1.4 \Lambda^*_{\ LL_-}, \tag{52}$$

as expected. The WCS configuration, not shown for clarity in Fig. 12, is only somewhat suppressed at lower energies, where the interference term is more important.

4 Conclusions

As we have discussed, the study of contact interactions at future colliders represents a *general* tool to hunt for traces of new physics (new heavy bosons,...) much above the available machine energy.

Fig. 13 contains a summary of the 'reach' Λ^* , as resulting from the various numerical analyses discussed in Sect. 3. The lengths of the white, black and white, and black bars denote the ranges of Λ^* values resulting for the standard helicity couplings of e^+e^-, eq and qq type contact terms, respectively.

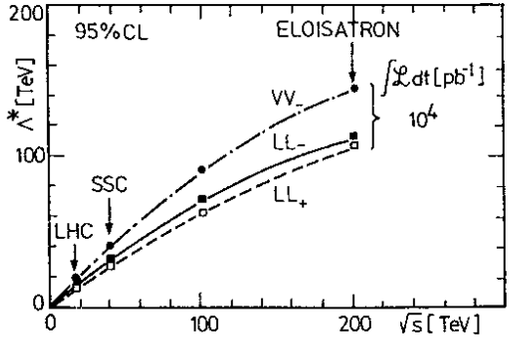

Figure 12: Λ^* at 95% CL versus $\sqrt{s}$ for various helicity couplings and pp colliders with $\int Ldt = 10^4\ pb^{-1}$.

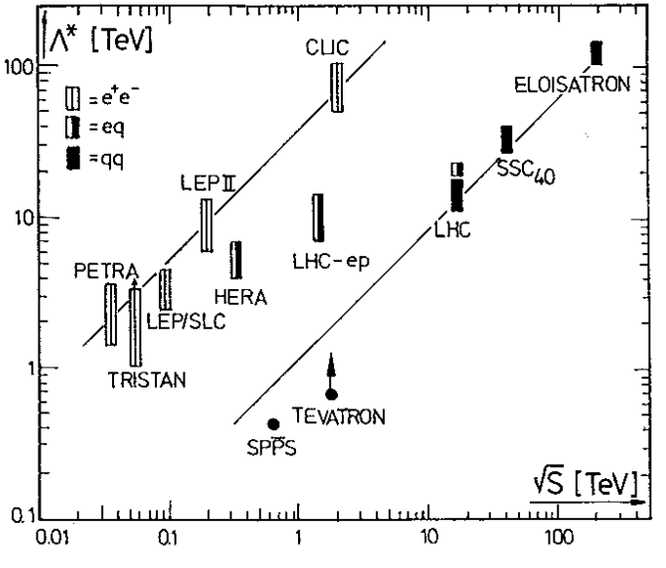

Figure 13: Summary of the 'reach' Λ^* at operating[17,26] and future pp, ep and e^+e^- machines. The two parallel lines are to guide the eye.

For instance, the 'reach' at the ELOISATRON may be expected to correspond to the one at CLIC. HERA ranges between LEP/SLC and LEP II. As explained, the 'reach' right on the Z^0 peak is exceptionally low.

The entries for PETRA, TRISTAN, $S\bar{p}pS$ and the TEVATRON correspond to actual experimental results[17,26] and fit well onto the general trend as a function of energy.

I wish to thank A. Ali for the pleasant and lively working atmosphere at the Erice Center, where this ELOISATRON workshop took place, G. Ingelman for providing me with a program for the nucleon structure functions, B. Naroska for experimental advice and, last not least, my wife Barbara for numerous helpful discussions and suggestions.

The support from the Deutsche Forschungsgemeinschaft until the end of 1988 is also acknowledged.

References

[1] for reviews see e.g
J. Ellis, Proc. 1985 Int. Symp. on Lepton and Photon Int.'s at High Energies, Kyoto/Japan;
D.V. Nanopoulos, Rivista del Nuovo Cimento 8 (1985) 1.

[2] for reviews see e.g.
W. Buchmüller, Schladming Lectures 1985, Acta Physica Austriaca, Suppl. XXVII (1985) 517;
F. Schrempp, MPI-Munich Report MPI-PAE/PTh 32/86, 1986 ('Habilitationsschrift').

[3] E. Eichten, K. Lane and M.E. Peskin, Phys. Rev. Lett. 50 (1983) 811.

[4] E. Eichten, I. Hinchliffe, K. Lane and C. Quigg, Rev. Mod. Phys. 56 (1984) 579; erratum, Fermilab-Pub-86-75 (1986).

[5] E. Eichten, Fermilab-Conf-85/178-T (1986).

[6] B. Schrempp, in "New Aspects of High-Energy Proton-Proton Collisions" (Ed. A. Ali, Plenum), 1989, p. 143.

[7] W. Buchmüller and D. Wyler, Nucl. Phys. B268 (1986) 621;
C.N. Leung, S.T. Love and S. Rao, Z. Phys. C31 (1986) 433.

[8] M. Chanowitz and M.K. Gaillard, Nucl. Phys. B261 (1985) 379
M. Chanowitz, M. Golden and H. Georgi, Phys. Rev. Lett. 57 (1986) 2344

[9] F. Schrempp, Proc. XXIII Int. Conf. on High Energy Physics, Berkeley/USA, 1986, Vol II, p. 1243.

[10] B. Schrempp, F. Schrempp, N. Wermes and D. Zeppenfeld, Nucl. Phys. B296 (1988) 1.

[11] U. Baur, A. Blondel, D. Bloch, D. Dominici, H. Fesefeld, K. Hamacher, L. Levinson, M. Lindner, L. Lyons, P. Mättig, P. Mery, E. Milotti, M. Perottet, F. Renard, D. Schildknecht, B. Schrempp, F. Schrempp, K.H. Schwarzer, D. Treille, N. Wermes and D. Zeppenfeld, Proc. ECFA Workshop on LEP200, Aachen, 1986, ECFA 87-108, 1987, Vol II, p. 414.

[12] B. Schrempp, unpublished.

[13] N. Wermes (B. Schrempp, F. Schrempp and D. Zeppenfeld), Proc. Workshop on Physics at Future Accelerators, La Thuile, CERN 87-07, 1987, Vol II, p. 305.

[14] HRS Collab., P. Baringer et al., Phys. Lett. B206 (1988) 551.

[15] B. Naroska, private communication.

[16] AMY Collab., A. Bacala et al., Phys. Lett. B218 (1989) 112

[17] UA1 Coll., G. Arnison et al., Phys. Lett B177 (1986) 244.

[18] A.K. Nandi, Proc. Workshop on Physics at Future Accelerators, La Thuile, CERN 87-07, 1987, Vol II, p. 270.

[19] R. Rückl, Phys. Lett. 129B (1983) 363; Nucl. Phys. B234 (1984) 91;
F. Cornet, Proc. 25th Int. Winter Meeting on Fundamental Physics, Sevilla/Spain, 1987, and DESY-Report 87-131 (1987).

[20] H.-U. Martyn, Proc. HERA Workshop, DESY, Hamburg/FRG, 1987, (Ed. R.D. Peccei), Vol II, p. 801.

[21] F. Cornet and R. Rückl, Proc. Workshop on Physics at Future Accelerators, La Thuile, CERN 87-07, 1987, Vol II, p. 287.

[22] UA2 Collab., P. Bagnaia et al., Phys. Lett. B138 (1984) 430.

[23] B.L. Combridge and C.J. Maxwell, Nucl. Phys. B239 (1984) 429.

[24] EHLQ1,2: Ref.[4];
DO1,2: D. Duke and J.F. Owens, Phys. Rev. D30 (1984) 49;
GHR: M. Glück, E. Hoffmann and E. Reya, Z. Phys. C13 (1982) 119;
MRS1,2,3: A.D. Martin, R.D. Roberts and J.Stirling, private communication by G. Ingelman.

[25] C.H. Llewellyn Smith, Proc. Second Hellenic Summer School, Corfu/Greece, 1985.

[26] PLUTO Collab., Ch. Berger et al., Z. Phys. C27 (1985) 341;
JADE Collab., W. Bartel et al., Z. Phys. C30 (1986) 371;
TASSO Collab., W. Braunschweig et al., Z. Phys. C40 (1988) 163;
HRS Collab., M. Derrick et al., Phys. Lett. B166 (1986);
MAC Collab., E. Fernandez et al., Phys. Rev. D35 (1987) 10;
M.J. Shochet, Proc. XXIV Int. Conf. on High Energy Physics, Munich/FRG, 1988 (Eds. R. Kotthaus and J.H. Kühn) p. 18.